Control of radial fingering patterns: A weakly nonlinear approach

Eduardo O. Dias and José A. Miranda*
Departamento de Física, LFTC, Universidade Federal de Pernambuco, Recife 50670-901, PE, Brazil
(Received 14 October 2009; published 15 January 2010)

It is well known that the constant injection rate flow in radial Hele-Shaw cells leads to the formation of highly branched patterns, where finger tip-splitting events are plentiful. Different kinds of patterns arise in the lifting Hele-Shaw flow problem, where the cell's gap width grows linearly with time. In this case, the morphology of the emerging structures is characterized by the strong competition among inward moving fingers. By employing a mode-coupling theory we find that both finger tip-splitting and finger competition can be restrained by properly adjusting the injection rate and the time-dependent gap width, respectively. Our theoretical model approaches the problem analytically and is capable of capturing these important controlling mechanisms already at weakly nonlinear stages of the dynamics.

DOI: 10.1103/PhysRevE.81.016312 PACS number(s): 47.15.gp, 47.54.−r, 47.20.Ma, 47.15.km

I. INTRODUCTION

The Saffman-Taylor instability [1] arises at the interface separating two viscous fluids constrained to flow in the narrow gap between closely spaced parallel plates of a Hele-Shaw cell. This famous pattern-forming problem [2] involves the development of stable smooth fingers in long rectangular channels or branched fronts if the flow takes place in an open radial geometry. Under radial flow circumstances [3–5] a less viscous fluid is radially injected into a more viscous one producing fingerlike structures which can split at their tips, tending toward a dense-branching morphology. The radial viscous fingering problem (Fig. 1) has been extensively studied during the last few decades, both experimentally [6–8] and theoretically [9–13].

Very recently, two research groups [14,15] have examined a still poorly explored aspect of the radial viscous fingering problem: the possibility of suppressing the emergence of the usual branched morphology, by properly controlling the injection rate of the less viscous fluid. In contrast to most previous investigations, instead of considering a constant injection process, they assumed a particular time-varying injection rate which scaled with time like $t^{-1/3}$. This procedure has been originally suggested by Bataille [3] who performed a linear stability analysis of the problem. However, under such time-dependent injection rate, the long-time evolution of the pattern-forming dynamics has been investigated in Refs. [14,15]. Their numerical and experimental findings for the fully nonlinear regime demonstrate that by continuously adjusting the injection rate the usual branched patterns are indeed suppressed and replaced with n-fold symmetric universal shapes. These results introduce a suggestive control technique which might improve the efficiency of a number of physical, biological, and engineering systems related to the radial viscous fingering phenomenon.

In this work we investigate control mechanisms in radial viscous fingering, but focus on a different time regime, and use an alternative theoretical strategy to attack the problem. Unlike previous studies which either addressed the early linear [3] or the fully advanced nonlinear time regimes [14,15], we tackle the problem by paying special attention to the dynamics that bridges these two extremes. We do this by considering the intermediate weakly nonlinear time stage. Moreover, instead of using purely linear stability analysis or intensive highly sophisticated numerical simulations, we approach the problem analytically through a second-order mode-coupling theory [9]. As opposed to conventional linear stability methods our weakly nonlinear study enables one to access the morphology of the emerging patterns. This theoretical procedure is valid and accurate at the onset of the nonlinear effects and gives insight into mechanisms of pattern control.

For the injection-driven radial fingering problem we show that finger tip splitting is suppressed, already at the weakly nonlinear stage, if the injection rate behaves as prescribed in Refs. [3,14,15]. We apply a similar maneuvering to demonstrate that fingering formation in time-dependent gap Hele-Shaw flows [16–20] can also be disciplined if one conveniently changes the lifting rate of the upper plate. In this case we show that finger competition is restrained if the gap width scales with time with exponent $-2/7$. In both cases mode-coupling theory provides mechanisms for the suppression of fingering, allowing the emergence of more symmetric structures. In this work we focus on the unstable situation in which the more viscous fluid is displaced by the less viscous one.

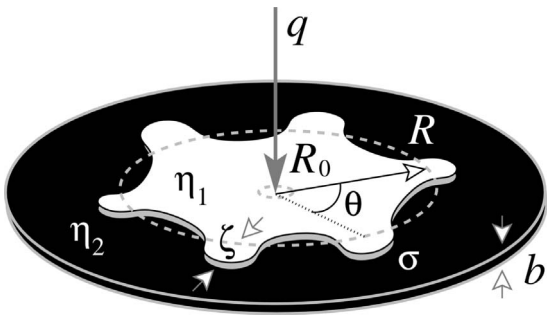

FIG. 1. Schematic setup for the injection-driven radial Hele-Shaw flow.

*jme@df.ufpe.br

II. INJECTION-DRIVEN HELE-SHAW FLOW

A. Mode-coupling approach

Consider a Hele-Shaw cell of constant gap spacing b containing two immiscible, incompressible, and viscous fluids (see Fig. 1). Denote the viscosities of the inner and outer fluids, respectively, as η_1 and η_2. Between the two fluids there exists a surface tension σ. Fluid 1 is injected into fluid 2 at a given injection rate $q=q(t)$ (equal to the area covered per unit time), which may depend on time. We describe the perturbed fluid-fluid interface as $\mathcal{R}(\theta,t)=R(t)+\zeta(\theta,t)$, where θ represents the azimuthal angle and $R(t)$ is the time-dependent unperturbed radius,

$$R(t)=\sqrt{R_0^2+\frac{1}{\pi}\int_0^t q(t')dt'}, \tag{1}$$

with R_0 being the unperturbed radius at $t=0$. The presence of the time integral in Eq. (1) is required since the injection rate is not necessarily constant. In addition, $\zeta(\theta,t)=\Sigma_{n=-\infty}^{+\infty}\zeta_n(t)\exp(in\theta)$ denotes the net interface perturbation with Fourier amplitudes $\zeta_n(t)$ and discrete azimuthal wave numbers $n=0,\pm 1,\pm 2,\ldots$. Our perturbative approach keeps terms up to the second order in ζ. In the Fourier expansion of ζ we include the $n=0$ mode to maintain the area of the perturbed shape independent of the perturbation ζ. Mass conservation imposes that the zeroth mode is written in terms of the other modes as $\zeta_0=-(1/2R)\Sigma_{n\neq 0}|\zeta_n(t)|^2$.

For the quasi-two-dimensional geometry of the Hele-Shaw cell, the flow velocity $\mathbf{v}_j=-\nabla\phi_j$, where ϕ_j represents the velocity potential in fluids $j=1,2$. The equation of motion of the interface is given by Darcy's law [1,2,5,9]

$$A\left(\frac{\phi_1+\phi_2}{2}\right)-\left(\frac{\phi_1-\phi_2}{2}\right)=-\frac{b^2(p_1-p_2)}{12(\eta_1+\eta_2)}, \tag{2}$$

where the dimensionless parameter $A=(\eta_2-\eta_1)/(\eta_2+\eta_1)$ is the viscosity contrast and p_j represents the hydrodynamic pressure.

To include the contributions coming from surface tension we consider a Young-Laplace pressure boundary condition, which expresses the pressure jump across the fluid-fluid interface,

$$p_1-p_2=\sigma\kappa, \tag{3}$$

where the interfacial curvature is denoted by κ. The problem is then specified by Eq. (3), plus the kinematic boundary condition, which states that the normal components of each fluid's velocity are continuous at the interface

$$\mathbf{n}\cdot\nabla\phi_1=\mathbf{n}\cdot\nabla\phi_2, \tag{4}$$

with $\mathbf{n}=\nabla[r-\mathcal{R}(\theta,t)]/|\nabla[r-\mathcal{R}(\theta,t)]|$ representing the unit normal vector at the interface.

For the injection-driven Hele-Shaw flow we consider the incompressibility condition

$$\nabla\cdot\mathbf{v}_j=0. \tag{5}$$

Under such circumstances, we define Fourier expansions for the velocity potentials, which obey Laplace's equation $\nabla^2\phi_j=0$. Then, we express ϕ_j in terms of the perturbation amplitudes ζ_n by considering condition (4). Substituting these relations, and the pressure jump condition (3) into Eq. (2), always keeping terms up to second order in ζ, and Fourier transforming, we find the dimensionless equation of motion for the perturbation amplitudes (for $n\neq 0$),

$$\dot{\zeta}_n=\lambda(n)\zeta_n+\sum_{n'\neq 0}[F(n,n')\zeta_{n'}\zeta_{n-n'}+G(n,n')\dot{\zeta}_{n'}\zeta_{n-n'}], \tag{6}$$

where the overdot denotes total time derivative,

$$\lambda(n)=\frac{Q(t)}{2\pi R^2}(A|n|-1)-\frac{1}{R^3}|n|(n^2-1) \tag{7}$$

is the linear growth rate, and

$$Q(t)=\frac{12q(t)(\eta_1+\eta_2)}{\sigma b} \tag{8}$$

is a dimensionless injection parameter. The second-order mode-coupling terms are given by

$$F(n,n')=\frac{|n|}{R}\left\{\frac{Q(t)A}{2\pi R^2}\left(\frac{1}{2}-\mathrm{sgn}(nn')\right)-\frac{1}{R^3}\left[1-\frac{n'}{2}(3n'+n)\right]\right\}, \tag{9}$$

$$G(n,n')=\frac{1}{R}\{A|n|[1-\mathrm{sgn}(nn')]-1\}. \tag{10}$$

The sgn function equals ± 1 according to the sign of its argument. In Eq. (6) lengths are rescaled by b and time by $[12b(\eta_1+\eta_2)]/\sigma$. For the remainder of this section, we work with the dimensionless version of the equations. We stress that the values we take for our dimensionless parameters are consistent with typical physical quantities used in real experiments for injection-driven radial viscous flow [2,3,5–8].

B. Suppression of finger tip splitting

We study a mechanism to control the finger shape behavior, by considering the coupling of a small number of modes. To simplify our discussion we rewrite Eq. (6) in terms of cosine and sine modes, where the cosine $a_n=\zeta_n+\zeta_{-n}$ and sine $b_n=i(\zeta_n-\zeta_{-n})$ amplitudes are real valued. Without loss of generality we choose the phase of the fundamental mode, so that $a_n>0$ and $b_n=0$. Under such circumstances, finger tip-sharpening and tip-splitting phenomena are described by considering the influence of a fundamental mode n on the growth of its harmonic $2n$ [9]. One key piece of information about the morphology of the emerging patterns can be extracted from the equation of motion for the harmonic cosine mode,

$$\dot{a}_{2n}=\lambda(2n)a_{2n}+\frac{1}{2}T(2n,n)a_n^2, \tag{11}$$

where the finger tip function is defined as

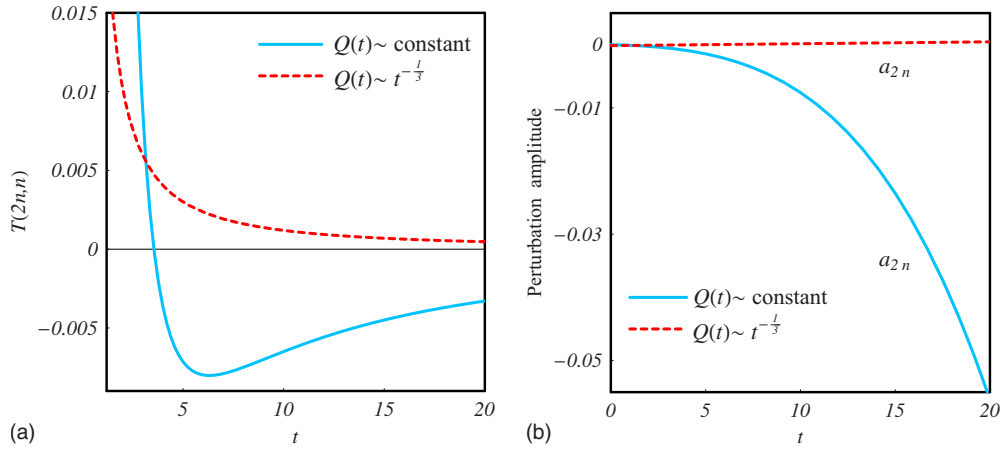

FIG. 2. (Color online) (a) Behavior of the finger tip function $T(2n,n)$ as time is varied, considering the coupling of modes $n=5$ and $2n=10$; (b) time evolution of the cosine perturbation amplitude for the first harmonic mode a_{2n}. The solid curves describe the situation at constant injection rate, while the dashed curves are plotted by taking a time-varying injection rate $Q=f(n,A)t^{-1/3}$. The constant injection rate is $Q=61.5$ and $f(5,1)=76.8$.

$$T(2n,n) = [F(2n,n) + \lambda(n)G(2n,n)]. \tag{12}$$

It can be shown that the equivalent growth of the sine mode b_{2n} is uninfluenced by a_n and does not present second-order couplings, so we focus on the growth of the cosine mode. The interesting point about the function $T(2n,n)$ is that it controls the finger shape behavior. The sign of $T(2n,n)$ dictates whether finger tip sharpening or finger tip splitting is favored by the dynamics. From Eq. (11) we see that, if $T(2n,n)>0$, the result is a driving term of order a_n^2 forcing growth of $a_{2n}>0$, the sign that is required to cause outward-pointing fingers to become sharp, favoring finger tip sharpening. In contrast, if $T(2n,n)<0$ the growth of $a_{2n}<0$ would be favored, leading to outward-pointing finger tip splitting.

To analyze the influence of the injection rate on the tip-splitting behavior at second order, in Fig. 2(a) we plot the behavior of $T(2n,n)$ as a function of time, for the coupling between two Fourier modes ($n=5$ and $2n=10$). This is done for the situations in which the injection rate is constant (solid curve), and also when it depends on time (dashed curve) as

$$Q(t) = f(n,A)t^{-1/3}, \tag{13}$$

where

$$f(n,A) = \left[\frac{8\pi^3(3n^2-1)^2}{3A^2}\right]^{1/3}. \tag{14}$$

A similar expression has been originally derived by Bataille [3]. Equation (13) can be obtained by using Eqs. (1) and (7) and by setting $d\lambda(n)/dn=0$. It provides the adequate injection rate needed to maintain the number of fingers n fixed and is equal to the fastest growing mode. For $Q(t)\sim$const, we observe that $T(2n,n)$ is initially positive, reaches zero, and then becomes negative. This describes the usual finger tip-splitting scenario: at early time stage the fingers look sharp, but as time progresses they become wider at their tips, which eventually tend to bifurcate. The situation is considerably different when the injection rate decreases with time as prescribed by Eq. (13): now, the finger tip function is always positive and assumes smaller magnitudes as time evolves. This indicates that the fingers will not be subjected to a tip-splitting process. Therefore, the patterns will retain their original n-fold symmetry as they grow.

In order to reinforce the conclusions reached from Fig. 2(a), in Fig. 2(b) we compare the time evolution of the cosine harmonic mode a_{2n} for both constant and time-varying injection rates. The initial perturbation amplitudes are $a_n(0)=0.1$ and $a_{2n}(0)=0$. We clearly observe that the weakly nonlinear coupling dictates the growth of the harmonic. For $Q(t)\sim$const the sign of the harmonic goes strongly negative although its initial value was zero. In this case, the nonlinear effects naturally enhance tendency toward finger tip splitting. On the other hand, when $Q\sim t^{-1/3}$ the amplitude of the harmonic mode does not change much with time and is always positive. This points to a nonlinear stabilization of the tip-splitting phenomenon induced by the nonlinear coupling between the harmonic mode and its fundamental.

The combined role of injection and nonlinear coupling in determining the finger tip behavior is even more clearly illustrated in Fig. 3 which plots the time evolution of the interface, plotted at equal time intervals Δt. Figure 3(a) is plotted for $0\le t\le 62.4$, $\Delta t=10.4$, and $\tau=62.5$, while in Fig. 3(b) we have $5\le t\le 905$, $\Delta t=150$, and $\tau=1790$. We consider the interaction of two representative cosine modes (a fundamental $n=5$ and its harmonic $2n=10$), for (a) $Q=61.5$ and (b) $Q(t)=f(5,1)t^{-1/3}$. Again, we take the initial amplitudes as $a_n(0)=0.1$ and $a_{2n}(0)=0$.

At this point we discuss our assessment of the largest time ($t=\tau$) for which our weakly nonlinear theoretical results are valid. We follow an approach originally proposed by Gingras and Rácz [21] for the linear regime and extend its range of applicability to the weakly nonlinear stage of evolution. While plotting the evolving interface we stop the time evolution of the patterns as soon as the base of the fingers starts to move inward, which would make successive interfaces to cross one another. Since this crossing is not observed in experiments [2,3,5–8], as in Ref. [21], we adopt the largest

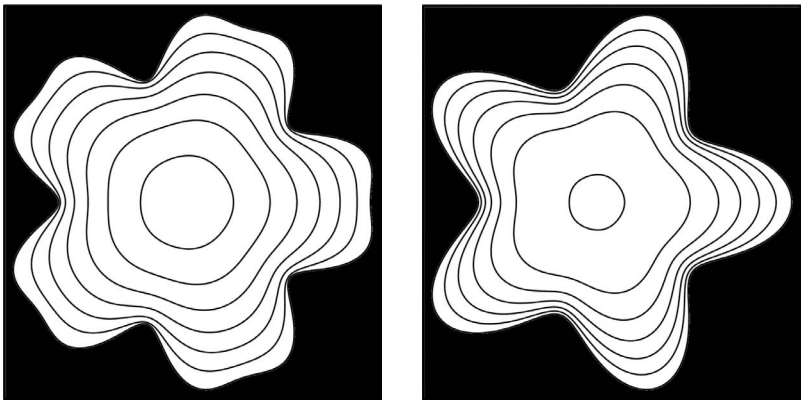

FIG. 3. Snapshots of the evolving interface, plotted at equal time intervals for the interaction of two cosine modes $n=5$ and $2n=10$ when (a) $Q(t)\sim$const and (b) $Q(t)=f(n,A)t^{-1/3}$. Here, the constant injection rate is $Q=61.5$ and $f(5,1)=76.8$. The area in black represents the more viscous fluid. Finger tip splitting is clearly present in (a) and suppressed in (b).

time before crossing as the upper bound time for the validity of our theoretical description. The usefulness and effectiveness of this criterion have been demonstrated in Ref. [21]. Thus, for the injection problem the instant when the interfacial velocity becomes negative for the first time gives an upper limit for the period in which the weakly nonlinear description is valid. This validity condition can be mathematically expressed as

$$\left[\frac{d\mathcal{R}}{dt}\right]_{t=\tau} = [\dot{R}(t) + \dot{\zeta}(\theta,t)]_{t=\tau} = 0. \tag{15}$$

Notice that, differently from what has been done in Ref. [21], we evaluate Eq. (15) by taking into account second-order contributions for interface perturbation $\zeta(\theta,t)$, as prescribed by our mode-coupling equation (6).

As one can see by examining Fig. 3(a) a constant injection rate leads to wide fingers, having blunt tips. At later times, these grown fingers clearly start to bifurcate, by splitting at their tips. This scenario is significantly changed when we consider a time-varying injection rate. In Fig. 3(b) we see a nearly circular initial interface evolving to a five-fingered structure. At later times, the resulting patterns are still fivefold symmetric, presenting the formation of fingering structures which show no tendency toward finger broadening and finger tip splitting. This is exactly the kind of behavior observed in Refs. [14,15] by performing experiments and simulations at the advanced time regime. Our mode-coupling weakly nonlinear analysis is able to capture this fully nonlinear stabilization process through relatively simple analytical means.

III. TIME-DEPENDENT GAP HELE-SHAW FLOW

A. Physical problem and mode-coupling description

A particularly interesting variation of the traditional radial Saffman-Taylor problem is the investigation of fingering instabilities in Hele-Shaw cells presenting variable gap spacing [16–20]. In such a "lifting" version of the radial fingering problem, the upper plate is lifted uniformly, while the lower plate remains at rest. During the lifting process the plates remain parallel to each other, so that the gap is a function of time, but not of space. Usually, the upper plate is moved at a constant lifting velocity V, so that the gap width grows linearly with time as $b(t)=b_0+Vt$, where b_0 is the initial plate-plate distance. This defines the conventional setup for time-dependent gap Hele-Shaw flows.

The uniform lifting forces the fluid-fluid interface to move inward forming visually striking fingering patterns. Initially, a circular droplet of the more viscous fluid undergoes a destabilization process via the penetration of multiple fingers of the outer less viscous fluid. The interface behavior is markedly characterized by the competition among the fingers of the invading less viscous fluid, which advance toward the center of the droplet. At the same time, it is also observed that the outermost limit of the interface ceases to shrink, indicating that the competition among the fingering structures of the more viscous fluid is considerably less intense.

In contrast to the injection-driven situation discussed in Sec. II where finger tip splitting is the prevalent pattern-forming mechanism, the most noteworthy morphological aspect in time-dependent gap Hele-Shaw flows is the strong competition among the penetrating fingering structures. In this section our main goal is to get analytical insight about the possibility of controlling such a finger competition process by properly manipulating the lifting rate of the upper plate.

The geometry of the time-dependent gap Hele-Shaw cell is sketched in Fig. 4. Consider a Hele-Shaw cell of a variable gap width $b(t)$ containing two immiscible, incompressible, and viscous fluids. The upper plate of the cell can be lifted along the direction perpendicular to the cell plates. On the other hand, the lower plate is held fixed. The initial fluid-fluid interface is circular, having radius R_0. By using volume

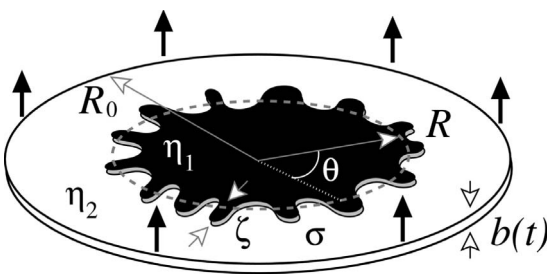

FIG. 4. Schematic setup for the time-dependent gap radial Hele-Shaw flow.

conservation the time-dependent radius of the unperturbed interface is given by

$$R(t) = R_0 \sqrt{\frac{b_0}{b(t)}}. \tag{16}$$

As in the case of the injection-driven flow, we use Darcy's law (2), the pressure jump condition (3), and the kinematic boundary condition (4) to obtain a differential equation for the perturbation amplitudes. However, due to the lifting of the upper plate, the gap-averaged incompressibility condition is now written as

$$\nabla \cdot \mathbf{v} = -\frac{\dot{b}(t)}{b(t)}, \tag{17}$$

so that the velocity potential obeys a Poisson equation

$$\nabla^2 \phi_j = \frac{\dot{b}(t)}{b(t)}. \tag{18}$$

Nevertheless, since the gap is only time dependent, the solution of Eq. (18) differs from the usual Laplacian only by the simple additional term $\bar{\phi}=\dot{b}r^2/(4b)$. Keeping this in mind, and by following the standard steps described in the injection-driven situation, a dimensionless mode-coupling equation of the form given by Eq. (6) can be obtained for the lifting Hele-Shaw case, where now

$$\lambda(n) = -\frac{\dot{b}}{2b}(A|n|+1) - \frac{8b^{7/2}}{\delta^3}|n|(n^2-1) \tag{19}$$

is the linear growth rate, and $\delta=2R_0/b_0$ denotes the initial aspect ratio. In addition, the second-order mode-coupling terms are given by

$$F(n,n') = \frac{\dot{b}}{b^{1/2}}\left[A|n|\left(\frac{1}{2} - \mathrm{sgn}(nn')\right) - 1\right] - \frac{16b^4}{\delta^3}|n|\left[1 - \frac{n'}{2}(3n'+n)\right], \tag{20}$$

$$G(n,n') = 2b^{1/2}\{A|n|[1-\mathrm{sgn}(nn')]-1\}. \tag{21}$$

Note that in Eqs. (19)–(21) in-plane lengths, $b(t)$, and time are rescaled by $2R_0$, b_0, and the characteristic time $T=[12b_0(\eta_1+\eta_2)]/\sigma$, respectively. Therefore, the dimensionless gap width is written as $b(t)=1+\beta t$, where $\beta=[12V(\eta_1+\eta_2)/\sigma]$. The dimensionless version of the equations is used throughout this section. As in Sec. II our dimensionless parameters are consonant with typical physical quantities used in real experiments for time-dependent gap radial viscous flow [17,19].

B. Inhibition of finger competition

We follow Refs. [9,20] and consider finger length variability as a measure of the competition among fingers. Within our approach the finger competition mechanism can be described by the influence of a fundamental mode n, assuming that n is even, on the growth of its subharmonic mode $n/2$. The equations of motion for the subharmonic mode can be written as

$$\dot{a}_{n/2} = \{\lambda(n/2) + C(n)a_n\}a_{n/2}, \tag{22}$$

$$\dot{b}_{n/2} = \{\lambda(n/2) - C(n)a_n\}b_{n/2}, \tag{23}$$

where the finger competition function is given by

$$C(n) = \frac{1}{2}\left[F\left(-\frac{n}{2},\frac{n}{2}\right) + \lambda(n/2)G\left(\frac{n}{2},-\frac{n}{2}\right)\right]. \tag{24}$$

Observing Eqs. (22) and (23) we verify that $C(n)>0$ increases the growth of the cosine subharmonic $a_{n/2}$, while inhibiting growth of its sine subharmonic $b_{n/2}$. The result is an increased variability among the lengths of fingers of fluid 1 invading the less viscous fluid 2. This effect describes the enhanced competition of the outward moving fingers of fluid 1. Sine modes $b_{n/2}$ would vary the lengths of fingers of fluid 2 penetrating into fluid 1, but it is clear from Eq. (23) that their growth is suppressed. Reversing the sign of $C(n)$ would exactly reverse these conclusions, such that modes $b_{n/2}$ would be favored over modes $a_{n/2}$. Therefore, $C(n)<0$ would indicate an increased competition among the inward moving fingers of fluid 2. Regardless of its sign, the magnitude of the function $C(n)$ measures the strength of the competition: increasingly larger values of $C(n)$ lead to an enhanced finger competition. The validity and correctness of this simple finger competition mechanism during advanced time stages have been extensively tested by numerical simulations [22,23].

To examine the influence of the time-dependent gap width on the finger competition behavior at second order, in Fig. 5(a) we plot the behavior of $C(n)$ as a function of time, for the coupling between two Fourier modes ($n=56$ and $n/2=28$). This is done for the situations in which the gap width grows linearly with time $b(t)=1+\beta t$ (solid curves), and also when it varies (dashed curves) as

$$b(t) = [1 + g(n,A,\delta)t]^{-2/7}, \tag{25}$$

where

$$g(n,A,\delta) = \left[\frac{56(3n^2-1)}{A\delta^3}\right]. \tag{26}$$

This expression can be obtained by using our Eq. (19) and setting $d\lambda(n)/dn=0$. Equation (25) provides the proper time-dependent gap width that is needed to maintain the number of fingers n fixed and equal to the fastest growing mode.

By examining Fig. 5(a) we observe that for these two different ways of lifting the upper plate, the finger competition function $C(n)$ only assumes negative values. This indicates that, for both cases, finger competition among inward moving fingers should be observed. However, it is also noticed that the magnitude of $C(n)$ is smaller when $b(t)$ is given by Eq. (25). This means that we should expect less intense finger competition events for this kind of lifting if compared with the usual situation in which $b(t)\sim t$.

The predictions made in Fig. 5(a) are supported by the results depicted in Fig. 5(b) which plots the time evolution of the sine ($b_{n/2}$) and cosine ($a_{n/2}$) subharmonic amplitudes

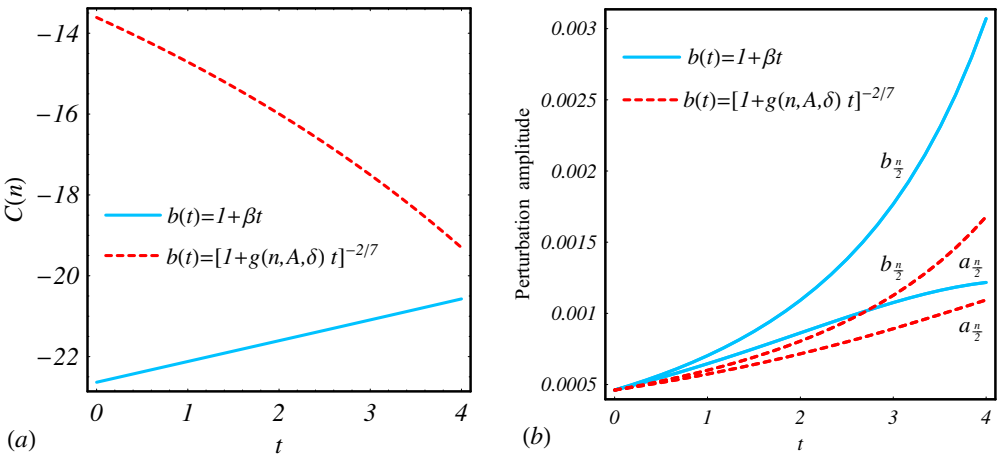

FIG. 5. (Color online) (a) Behavior of the finger competition function $C(n)$ as time is varied; (b) time evolution of the cosine ($a_{n/2}$) and sine ($b_{n/2}$) perturbation amplitudes for the subharmonic mode. The solid curves describe the situation where $b(t)=1+\beta t$, with $\beta=0.03$. The dashed curves are plotted by assuming that $b(t)=[1+g(n,A,\delta)t]^{-2/7}$, where $g(56,-1,200)=0.066$.

for $b(t)=1+\beta t$ (solid curves) and $b(t)=[1+g(n,A,\delta)t]^{-2/7}$ (dashed curves). We take the initial amplitudes as $a_{n/2}(0)=b_{n/2}(0)=0.000\,46$ and $a_n(0)=0.0013$. Recall that the finger length variability and the very nature of finger competition (i.e., among inward or outward moving fingers) depend on the relative magnitudes of cosine and sine subharmonic amplitudes. From Fig. 5(b) it is evident that the growth of $b_{n/2}$ over $a_{n/2}$ is significantly diminished when $b(t)=[1+g(n,A,\delta)t]^{-2/7}$, meaning that a restrained finger competition should occur.

The inhibition effect discussed above is further illustrated in Fig. 6 which shows the fluid-fluid interface at time $t=4$ considering the same initial conditions and physical parameters used in Fig. 5(b). We point out that for the lifting problem the largest allowed time τ, which can also be calculated from Eq. (15), indicates the transition from negative (inward motion) to positive (outward motion) interfacial velocity. The time $\tau=4$ [$\tau=5.3$] for the situation depicted in Fig. 6(a) [Fig. 6(b)]. Figure 6(a) exhibits the interface when $b(t)=1+\beta t$, revealing the competition among inward moving fingers. On the other hand, Fig. 6(b) illustrates the interface obtained when $b(t)=[1+g(n,A,\delta)t]^{-2/7}$, in which the competition among inward moving fingers is damped, resulting in a more in-and-out symmetric pattern.

IV. CONCLUSION

Injection-driven flow in radial Hele-Shaw cells results in highly ramified patterns if the injection rate is constant in time. The emerging structures are markedly characterized by the occurrence of finger tip-splitting events. Likewise, time-dependent gap flow in lifting Hele-Shaw cells leads to complex pattern morphologies if the cell's gap width grows linearly with time. In this case, the resulting shapes are formed due to the intense competition among the fingered structures. In this work, we have explored the possibility of controlling the development of both finger tip splitting and finger competition by properly manipulating the injection and the lifting rates.

In contrast to previous investigations [14,15] which examined controlling mechanisms during fully nonlinear stages of pattern evolution for the injection-driven problem, we focused on the onset of nonlinear effects. Instead of relying on meticulous experiments or sophisticated numerical simulations, we used a relatively simple weakly nonlinear approach. Despite its simplicity, our theoretical model was capable of extracting important analytical information about the possibility of inhibiting the appearance of complex interfacial features not only in the injection-driven situation, but also in variable gap width Hele-Shaw flows.

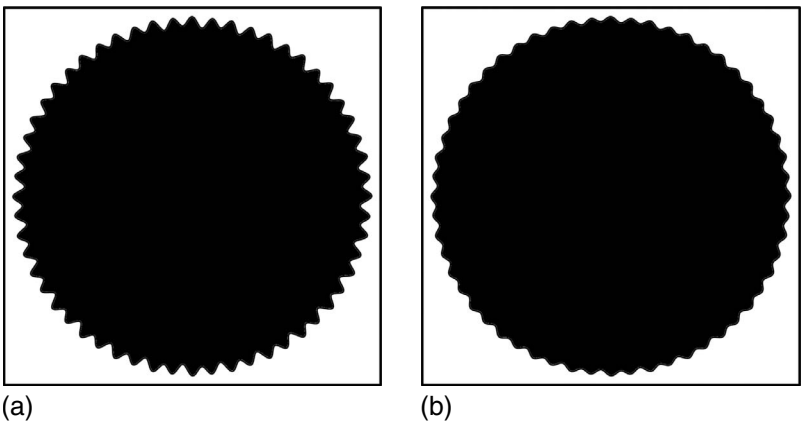

FIG. 6. Snapshot of the fluid-fluid interface at time $t=4$ for the interaction of two modes $n=56$ and $n/2=28$ (both sine and cosine) when (a) $b(t)=1+\beta t$, with $\beta=0.03$, and (b) $b(t)=[1+g(n,A,\delta)t]^{-2/7}$, where $g(56,-1,200)=0.066$. The area in black represents the more viscous fluid. Finger competition among inward moving fingers is detected in (a) and inhibited in (b).

Our analysis indicates that the control of finger tip splitting in injection-driven flow can be understood simply through the coupling between two modes: the fundamental and its harmonic. Under such circumstances, a time-dependent injection rate $Q(t) \sim t^{-1/3}$ would lead to the suppression of the branching morphology through the damping of the harmonic perturbation. Similarly, we have verified that the determination of a controlling mechanism for finger competition in lifting Hele-Shaw flows could be also be achieved via a two-mode mechanism, now involving the fundamental and its subharmonic. In this case, if the gap width varies in time with a $-2/7$ exponent, finger competition is made unfavorable by means of the inhibited growth of subharmonic perturbations. By employing these procedures quite symmetric interfacial patterns are obtained, where branching and competition phenomena are clearly restrained. These suggestive findings indicate that such important controlling mechanisms can be caught and predicted already at weakly nonlinear time stages of the pattern evolution. In conclusion, realistic predictions are obtained for the morphology of the patterns without recourse to intensive numerical calculations.

ACKNOWLEDGMENTS

J.A.M. thanks CNPq (Brazilian Research Council) for financial support of this research through the program "Instituto Nacional de Ciência e Tecnologia de Fluidos Complexos (INCT-FCx)," and also through the CNPq/FAPESQ Pronex program. E.O.D. wishes to thank CNPq for financial support. We gratefully acknowledge helpful discussions with Hélio M. Lins.

[1] P. G. Saffman and Geoffrey Taylor, Proc. R. Soc. London, Ser. A **245**, 312 (1958).
[2] For review papers, see, for instance, G. Homsy, Annu. Rev. Fluid Mech. **19**, 271 (1987); K. V. McCloud and J. V. Maher, Phys. Rep. **260**, 139 (1995); J. Casademunt, Chaos **14**, 809 (2004).
[3] J. Bataille, Rev. Inst. Fr. Pet. Ann. Combust. Liq. **23**, 1349 (1968).
[4] S. D. R. Wilson, J. Colloid Interface Sci. **51**, 532 (1975).
[5] L. Paterson, J. Fluid Mech. **113**, 513 (1981).
[6] J.-D. Chen, J. Fluid Mech. **201**, 223 (1989); Exp. Fluids **5**, 363 (1987).
[7] H. Thomé, M. Rabaud, V. Hakim, and Y. Couder, Phys. Fluids A **1**, 224 (1989).
[8] O. Praud and H. L. Swinney, Phys. Rev. E **72**, 011406 (2005).
[9] J. A. Miranda and M. Widom, Physica D **120**, 315 (1998).
[10] P. Fast and M. J. Shelley, J. Comput. Phys. **212**, 1 (2006).
[11] J. Mathiesen, I. Procaccia, H. L. Swinney, and M. Thrasher, EPL **76**, 257 (2006).
[12] S. W. Li, J. S. Lowengrub, and P. H. Leo, J. Comput. Phys. **225**, 554 (2007).
[13] C.-Y. Chen, C.-W. Huang, H. Gadêlha, and J. A. Miranda, Phys. Rev. E **78**, 016306 (2008).
[14] S. W. Li, J. S. Lowengrub, J. Fontana, and P. Palffy-Muhoray, Phys. Rev. Lett. **102**, 174501 (2009).
[15] A. Leshchiner, M. Thrasher, M. B. Mineev-Weinstein, and H. L. Swinney, Phys. Rev. E **81**, 016206 (2010).
[16] M. J. Shelley, F.-R. Tian, and K. Wlodarski, Nonlinearity **10**, 1471 (1997).
[17] D. Derks, A. Lindner, C. Creton, and D. Bonn, J. Appl. Phys. **93**, 1557 (2003).
[18] C.-Y. Chen, C.-H. Chen, and J. A. Miranda, Phys. Rev. E **71**, 056304 (2005).
[19] A. Lindner, D. Derks, and M. J. Shelley, Phys. Fluids **17**, 072107 (2005).
[20] E. O. Dias and J. A. Miranda, Phys. Rev. E **80**, 026303 (2009).
[21] M. J. P. Gingras and Z. Rácz, Phys. Rev. A **40**, 5960 (1989).
[22] J. A. Miranda and E. Alvarez-Lacalle, Phys. Rev. E **72**, 026306 (2005).
[23] C.-Y. Chen, C.-H. Chen, and J. A. Miranda, Phys. Rev. E **73**, 046306 (2006).